5 Dynamic response and effective static load distributions

5.1 Introduction

Due to the turbulent nature of the wind velocities in storms of all types, the wind loads acting on structures are also highly fluctuating. There is a potential to excite resonant dynamic response for structures, or parts of structures, with natural frequencies less than about 1 Hz. The resonant response of a structure introduces the complication of a time-history effect, in which the response at any time depends not just on the instantaneous wind gust velocities acting along the structure, but also on the previous time history of wind gusts.

This chapter will introduce the principles and analysis of dynamic response to wind. Some discussion of aeroelastic and fatigue effects is included. Also in this chapter, the method of equivalent or effective static wind loading distributions is introduced.

Treatment of dynamic response is continued in Chapters 9 to 12 on tall buildings, large roofs and sports stadiums, slender towers and masts, and bridges, with emphasis on the particular characteristics of these structures. In Chapter 15 code approaches to dynamic response are considered.

5.2 Principles of dynamic response

The fluctuating nature of wind velocities, pressures and forces, as discussed in Chapters 3 and 4, may cause the excitation of significant resonant vibratory response in structures or parts of structures, provided their natural frequencies and damping are low enough. This resonant dynamic response should be distinguished from the background fluctuating response to which all structures are subjected. Figure 5.1 shows the response spectral

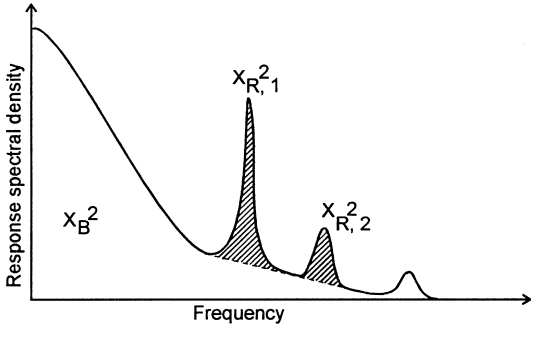

Figure 5.1 Response spectral density for a structure with significant resonant contributions.

density of a dynamic structure under wind loading; the area under the entire curve represents the total mean-square fluctuating response (note that the mean response is not included in this plot). The resonant responses in the first two modes of vibration are shown hatched in this diagram. The background response, made up largely of low-frequency contributions below the lowest natural frequency of vibration, is the largest contributor in Figure 5.1, and, in fact, is usually the dominant contribution in the case of along-wind loading. Resonant contributions become more and more significant, and will eventually dominate, as structures become taller or longer in relation to their width, and their natural frequencies become lower and lower.

Figure 5.2(a) shows the characteristics of the time histories of an along-wind (drag) force; the structural response for a structure with a *high* fundamental natural frequency is shown in Figure 5.2(b), and the response with a *low* natural frequency in Figure 5.2(c). In the former case, the resonant, or vibratory component, clearly plays a minor role in the response, which generally follows closely the time variation of the exciting forces. However, in the latter case, the resonant response, in the fundamental mode of vibration, is important, although response in higher modes than the first can usually be neglected.

In fact, the majority of structures fall into the category of Figure 5.2(b), and will *not* experience significant resonant dynamic response. A well known rule of thumb is that the lowest natural frequency should be below 1 Hz for the resonant response to be significant. However the amount of resonant response also depends on the damping, aerodynamic or structural, present. For example, high voltage transmission lines usually have fundamental sway frequencies which are well below 1 Hz; however, the *aerodynamic* damping is very high – typically around 25% of critical – so that the resonant response is largely damped out. Lattice towers, because of their low mass, also have high aerodynamic damping ratios. Slip jointed steel lighting poles have high *structural* damping due to friction at the joints – this energy absorbing mechanism will limit the resonant response to wind.

Resonant response, when it does occur, may occasionally produce complex interactions, in which the movement of the structure itself results in additional aeroelastic forces being produced (Section 5.5). In some extreme cases, for example the Tacoma Narrows Bridge failure of 1940 (see Chapter 1), catastrophic failure has resulted. These are exceptional cases, which of course must be avoided, but in the majority of structures with significant resonant dynamic response, the dynamic component is superimposed on a significant or dominant mean and background fluctuating response.

The two major sources of fluctuating wind loads are discussed in Section 4.6. The first and obvious source, exciting resonant dynamic response, is the natural unsteady or turbulent flow in the wind, produced by shearing actions as the air flows over the rough surface of the earth, as discussed in Chapter 3. The other main source of fluctuating loads is the alternate vortex shedding which occurs behind bluff cross-sectional shapes, such as circular cylinders or square cross-sections. A further source are buffeting forces from the wakes of other structures upwind of the structure of interest.

When a structure experiences resonant dynamic response, counteracting structural forces come into play to balance the wind forces:

- inertial forces proportional to the mass of the structure
- damping or energy-absorbing forces – in their simplest form, these are proportional to the velocity, but this is not always the case
- elastic or stiffness forces proportional to the deflections or displacements.

When a structure does respond dynamically, i.e. the resonant response is significant, an

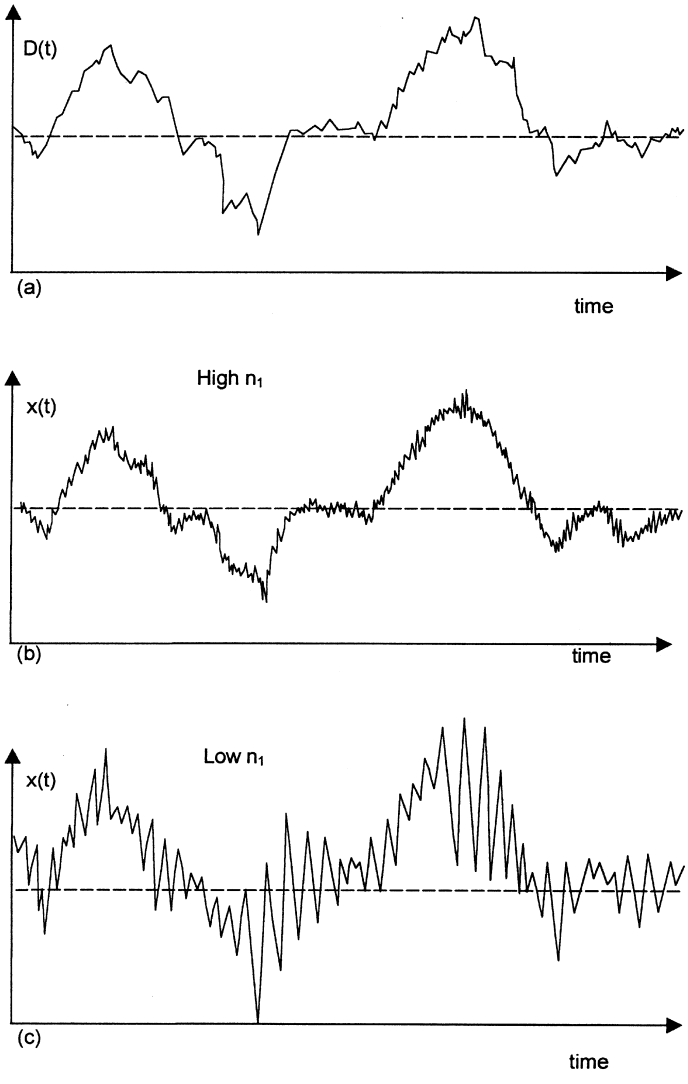

Figure 5.2 Time histories of: (a) wind force, (b) response of a structure with a high natural frequency and (c) response of a structure with a low natural frequency.

important principle to remember is that the condition of the structure, i.e. stresses, deflections, at any given time depends not only on the wind forces acting at the time, but also on the *past history* of wind forces. In the case of quasi-static loading, the structure responds directly to the forces acting instantaneously at any given time.

The effective load distribution due to the resonant part of the loading (Section 5.4.4) is given to a good approximation by the distribution of inertial forces along the structure. This is based on the assumption that the fluctuating wind forces at the resonant frequency approximately balance the damping forces once a stable amplitude of vibration is established.

At this point, it is worth noting the essential differences between dynamic response of structures to wind and earthquake. The main differences between the excitation forces due to these two natural phenomena are:

- Earthquakes are of much shorter duration than windstorms (with the possible exception of the passage of a tornado), and are thus treated as transient loadings.
- The predominant frequencies of the earthquake ground motions are typically 10–50 times those of the frequencies in fully-developed windstorms. This means that structures will be affected in different ways, e.g. buildings in a certain height range may not experience significant dynamic response to wind loadings, but may be prone to earthquake excitation.
- The earthquake ground motions will appear as *fully*-correlated equivalent forces acting over the height of a tall structure. However, the eddy structure in windstorms results in *partially*-correlated wind forces acting over the height of the structure. Vortex-shedding forces on a slender structure also are not full correlated over the height.

Figure 5.3 shows the various frequency ranges for excitation of structures by wind and earthquake actions.

5.3 The random vibration or spectral approach

In some important papers in the 1960s, A. G. Davenport outlined an approach to the wind-induced vibration of structures based on random vibration theory (Davenport, 1961, 1963, 1964). Other significant early contributions to the development of this approach were made by R. I. Harris (1963) and B. J. Vickery (1965, 1966).

The approach uses the concept of the stationary random process to describe wind velocities, pressures and forces. This assumes that the complexities of nature are such that we can never describe, or predict, perfectly (or 'deterministically') the forces generated by windstorms. However, we are able to use averaged quantities like standard deviations,

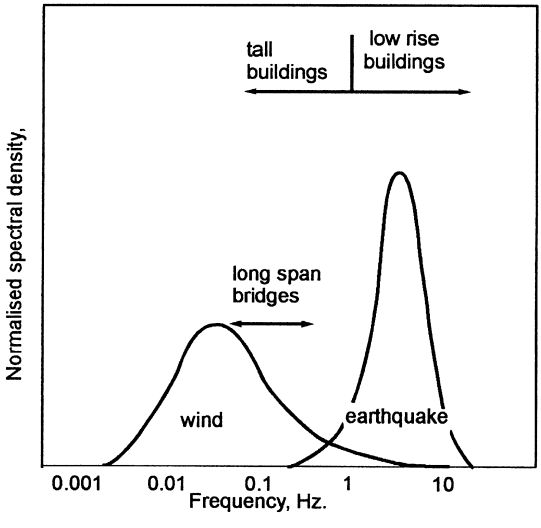

Figure 5.3 Dynamic excitation frequencies of structures by wind and earthquake.

correlations and spectral densities (or 'spectra') to describe the main features of both the exciting forces and the structural response. The *spectral density*, which has already been introduced in Section 3.3.4 and Figure 5.1, is the most important quantity to be considered in this approach, which primarily uses the *frequency domain* to perform calculations, and is alternatively known as the *spectral approach*.

Wind speeds, pressures and resulting structural response have generally been treated as stationary random processes in which the time-averaged or mean component is separated from the fluctuating component. Thus:

$$\bar{X}(t) = \bar{X} + x'(t) \tag{5.1}$$

where $X(t)$ denotes either a wind velocity component, a pressure (measured with respect to a defined reference static pressure), or a structural response such as bending moment, stress resultant, deflection, etc; $\bar{X}$ is the mean or time-averaged component; and $x'(t)$ is the fluctuating component such that $\overline{x'(t)} = 0$. If x is a response variable, $x'(t)$ should include any resonant dynamic response resulting from excitation of any natural modes of vibration of the structure.

Figure 5.4 (after Davenport, 1963) illustrates graphically the elements of the spectral approach. The main calculations are done in the bottom row, in which the total mean square fluctuating response is computed from the spectral density, or 'spectrum', of the response. The latter is calculated from the spectrum of the aerodynamic forces, which are, in turn, calculated from the wind turbulence, or gust spectrum. The frequency-dependent *aerodynamic* and *mechanical admittance* functions form links between these spectra. The amplification at the resonant frequency, for structures with a low fundamental frequency, will result in a higher mean square fluctuating and peak response, than is the case for structures with a higher natural frequency, as previously illustrated in Figure 5.2.

The use of stationary random processes and equation (5.1) is appropriate for large-scale windstorms such as gales in temperate latitudes and tropical cyclones. It may not

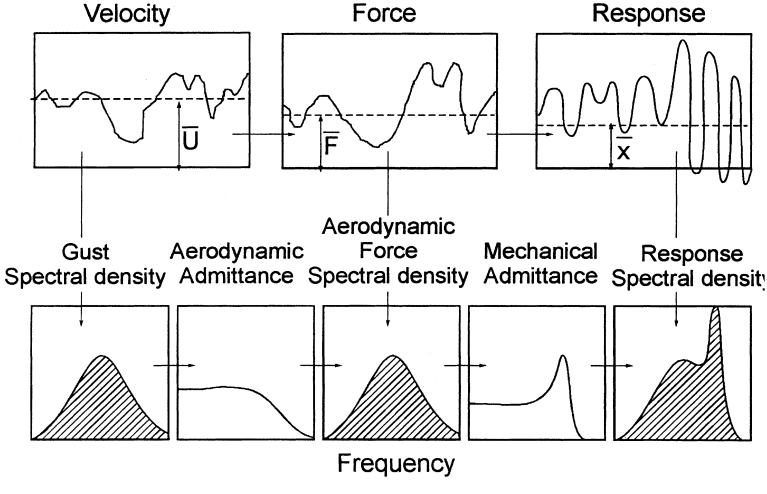

Figure 5.4 The random vibration (frequency domain) approach to resonant dynamic response (Davenport, 1963).

be appropriate for some short-duration, transient storms, such as downbursts or tornadoes associated with thunderstorms. Methods for these types of storms are still under development.

5.3.1 Along-wind response of a single-degree-of-freedom structure

We will consider first the along-wind dynamic response of a small body, whose dynamic characteristics are represented by a simple mass-spring-damper (Figure 5.5), and which does not disturb the approaching turbulent flow significantly. This is a single-degree-of freedom system, and is reasonably representative of a structure consisting of a large mass supported by a column of low mass, such as a lighting tower or mast with a large array of lamps on top.

The equation of motion of this system under an aerodynamic drag force, $D(t)$, is given by equation (5.2)

$$m\ddot{x} + c\dot{x} + kx = D(t) \tag{5.2}$$

The quasi-steady assumption (Section 4.6.2) for small structures allows the following relationship between mean square fluctuating drag force, and fluctuating longitudinal wind velocity to be written.

$$\overline{D^{\cdot 2}} = C_{Do}{}^2\rho^2\bar{U}^2\overline{u'^2}A^2 \cong \bar{C}_D{}^2\rho^2\bar{U}^2\overline{u'^2}A^2 = \frac{4\bar{D}^2}{\bar{U}^2}\overline{u'^2} \tag{5.3}$$

Equation (5.3) is analogous to equation (4.15) for pressures.

Writing equation (5.3) in terms of spectral density,

Hence,

$$\int_0^\infty S_D(n).dn = \frac{4\bar{D}^2}{\bar{U}^2}\int_0^\infty S_u(n).dn$$

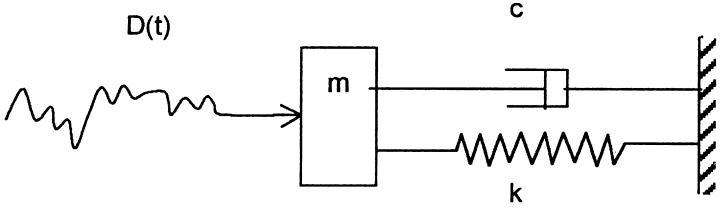

$$n_1 = \frac{1}{2\pi}\sqrt{\frac{k}{m}} \qquad \eta = \frac{c}{2\sqrt{mk}}$$

Figure 5.5 Simplified dynamic model of a structure.

$$S_D(n) = \frac{4\bar{D}^2}{\bar{U}^2} S_u(n) \tag{5.4}$$

To derive the relationship between fluctuating force, and the response of the structure, represented by the simple dynamic system of Figure 5.5, the deflection is first separated into mean and fluctuating components, as in equation (5.1):

$$X(t) = \bar{X} + x'(t) \tag{5.1}$$

The relationship between mean drag force, $\bar{D}$, and mean deflection, $\bar{X}$, is as follows:

$$\bar{D} = k\,\bar{X} \tag{5.5}$$

where k is the spring stiffness in Figure 5.5.

The spectral density of the deflection is related to the spectral density of the applied force as follows:

$$S_x(n) = \frac{1}{k^2} |H(n)|^2 S_D(n) \tag{5.6}$$

where $|H(n)|^2$ is known as the *mechanical admittance* for the single-degree-of-freedom dynamic system under consideration, given by equation (5.7).

$$|H(n)|^2 = \frac{1}{\left[1 - \left(\frac{n}{n_1}\right)^2\right]^2 + 4\eta^2\left(\frac{n}{n_1}\right)^2} \tag{5.7}$$

$|H(n)|$, i.e. the square root of the mechanical admittance, may be recognized as the *dynamic amplification factor*, or *dynamic magnification factor*, which arises when the response of a single-degree-of-freedom system to a harmonic, or sinusoidal, excitation force is considered. n_1 is the undamped natural frequency, and η is the ratio of the damping coefficient, c, to critical damping, as shown in Figure 5.5.

By combining equations (5.4) and (5.6), the spectral density of the deflection response can be related to the spectral density of the wind velocity fluctuations.

$$S_x(n) = \frac{1}{k^2} |H(n)|^2 \frac{4\bar{D}^2}{\bar{U}^2} S_u(n) \tag{5.8}$$

Equation (5.8) applies to structures which have small frontal areas in relation to the length scales of atmospheric turbulence.

For larger structures, the velocity fluctuations do not occur simultaneously over the windward face and their correlation over the whole area, A, must be considered. To allow for this effect, an *aerodynamic admittance*, $\chi^2(n)$, is introduced.

$$S_x(n) = \frac{1}{k^2} |H(n)|^2 \frac{4\bar{D}^2}{\bar{U}^2} . \chi^2(n) . S_u(n)$$

Substituting for $\bar{D}$ from equation (5.5),

$$S_x(n) = \frac{4\bar{X}^2}{\bar{U}^2}|H(n)|^2.\chi^2(n).S_u(n) \tag{5.9}$$

For open structures, such as lattice frame towers, which do not disturb the flow greatly, $\chi^2(n)$ can be determined from the correlation properties of the upwind velocity fluctuations (see Section 3.3.6). This assumption is also made for solid structures, but $\chi^2(n)$ has also been obtained experimentally.

Figure 5.6 shows some experimental data with an empirical function fitted. Note that $\chi(n)$ tends towards 1.0 at low frequencies and for small bodies. The low frequency gusts are nearly fully correlated, and fully envelope the face of a structure. For high frequencies, or very large bodies, the gusts are ineffective in producing total forces on the structure, due to their lack of correlation, and the aerodynamic admittance tends towards zero.

To obtain the mean square fluctuating deflection, the spectral density of deflection, given by equation (5.8), is integrated over all frequencies.

$$\sigma_x^2 = \int_0^\infty S_x(n).dn = \int_0^\infty \frac{4\bar{X}^2}{\bar{U}^2}|H(n)|^2.\chi^2(n).S_u(n).dn \tag{5.10}$$

The area underneath the integrand in equation (5.10) can be approximated by two components, B and R, representing the 'background' and resonant parts, respectively (Figure 5.7).

Thus,

$$\sigma_x^2 = \frac{4\bar{X}^2\sigma_u^2}{\bar{U}^2}\int_0^\infty |H(n)|^2.\chi^2(n).\frac{S_u(n)}{\sigma_u^2}.dn \cong \frac{4\bar{X}^2\sigma_u^2}{\bar{U}^2}[B + R] \tag{5.11}$$

where,

$$B = \int_0^\infty \chi^2(n).\frac{S_u(n)}{\sigma_u^2}.dn \tag{5.12}$$

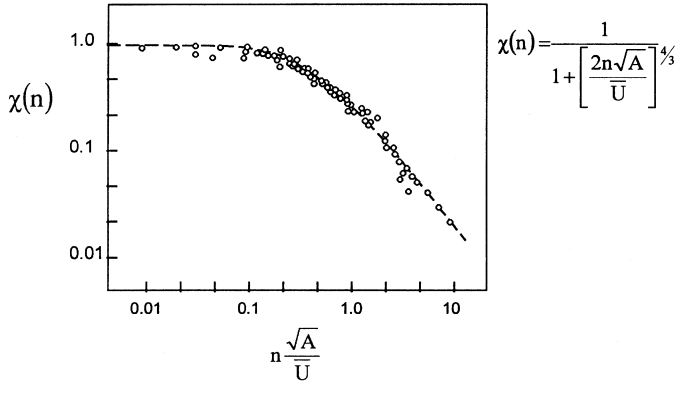

Figure 5.6 Aerodynamic admittance – experimental data and fitted function (Vickery, 1965).

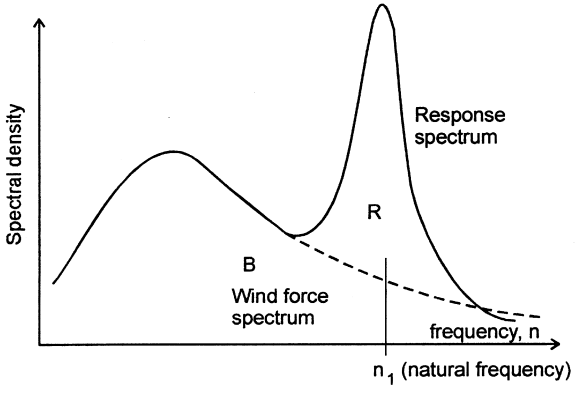

Figure 5.7 Background and resonant components of response.

$$R = \chi^2(n_1).\frac{S_u(n_1)}{\sigma_u^{\,2}}\int_0^{\infty}|H(n)|^2.dn \tag{5.13}$$

The approximation of equation (5.11) is based on the assumption that over the width of the resonant peak in Figure 5.7, the functions $\chi^2(n)$, $S_u(n)$ are constant at the values $\chi^2(n_1)$, $S_u(n_1)$. This is a good approximation for the flat spectral densities characteristic of wind loading, and when the resonant peak is narrow, as occurs when the damping is low (Ashraf Ali and Gould, 1985). The integral $\int|H(n)|^2.dn$ integrated for n from 0 to ∞, can be evaluated by the method of poles (Crandall and Mark, 1963) and shown to be equal to $(\pi n_1/4\eta)$.

The approximation of equation (5.11) is used widely in code methods of evaluating along-wind response, and will be discussed further in Chapter 15.

The background factor, B, represents the quasi-static response caused by gusts below the natural frequency of the structure. Importantly, it is independent of frequency, as shown by equation (5.12), in which the frequency appears only in the integrand, and thus is 'integrated out'. For many structures under wind loading, B is considerably greater than R, i.e. the background response is dominant in comparison with the resonant response. An example of such a structure is that whose response is shown in Figure 5.2(b).

5.3.2 Gust response factor

A commonly used term in wind engineering is *gust response factor*. The term *gust loading factor* was used by Davenport (1967), and *gust factor* by Vickery (1966). These essentially have the same meaning, although sometimes the factor is applied to the effective applied loading, and sometimes to the response of the structure. The term 'gust factor' is better applied to the wind speed itself (Section 3.3.3).

The *gust response factor*, G, may be defined as the ratio of the expected maximum response (e.g. deflection or stress) of the structure in a defined time period (e.g. 10 min or 1 h), to the mean, or time-averaged response, in the same time period. It really only has meaning in stationary or near-stationary winds such as those generated by large scale

synoptic wind events such as gales from depressions in temperate latitudes, or tropical cyclones (see Chapter 2).

The expected maximum response of the simple system described in Section 5.3.1 can be written:

$$\hat{X} = \bar{X} + g\sigma_x$$

where g is a *peak factor*, which depends on the time interval for which the maximum value is calculated, and the frequency range of the response.

From equation (5.11),

$$G = \frac{\hat{X}}{\bar{X}} = 1 + g\frac{\sigma_x}{\bar{X}} = 1 + 2g\frac{\sigma_u}{\bar{U}}\sqrt{B + R} \tag{5.14}$$

Equation (5.14), or variations of it, are used in many codes and standards for wind loading, for simple estimations of the along-wind dynamic loading of structures. The usual approach is to calculate G for the modal coordinate in the first mode of vibration, a_1, and then to apply it to a mean load distribution on the structure, from which all responses, such as bending moments, are calculated. This is an approximate approach which works reasonably well for some structures and load effects, such as the base bending moment of tall buildings. However in other cases it gives significant errors and should be used with caution (e.g. Holmes, 1994; Vickery, 1995 – see also Chapter 11).

5.3.3 Peak factor

The along-wind response of structures to wind has a probability distribution which is closely Gaussian. For this case, Davenport (1964) derived the following expression for the peak factor, g.

$$g = \sqrt{2\log_e(\nu T)} + \frac{0.577}{\sqrt{2\log_e(\nu T)}} \tag{5.15}$$

where ν is the 'cycling rate' or effective frequency for the response; this is often conservatively taken as the natural frequency, n_1. T is the time interval over which the maximum value is required.

5.3.4 Dynamic response factor

In transient or non-stationary winds such as downbursts from thunderstorms, for example, the use of a gust factor, or gust response factor, is meaningless. The gust response factor is also meaningless in cases when the mean response is very small or zero (such as cross-wind response). In these cases, use of a 'dynamic response factor' is more appropriate. This approach has been adopted recently in some codes and standards for wind loading. The dynamic response factor may be defined in the following way:

> Dynamic response factor = (maximum response including resonant and correlation effects)/(maximum response calculated ignoring both resonant and correlation effects)

The denominator is in fact the response calculated using 'static' methods in codes and standards. The dynamic response factor defined as above, will usually have a value close to 1. A value greater than 1 can only be caused by a significant resonant response.

The use of the gust response factor and dynamic response factor in wind loading codes and standards, will be discussed further in Chapter 15.

5.3.5 Influence coefficient

When considering the action of a time-dependent and spatially varying load such as wind loading on a continuous structure, the *influence coefficient* or *influence line* is an important parameter. To appreciate the need for this, we must understand the concept, familiar to structural designers, of 'load effect'. A load effect is not the load itself but a parameter resulting from the loading which is required for comparison with design criteria. Examples are internal forces or moments such as bending moments or shear forces, stresses or deflections. The influence line represents the value of a single load effect as a unit (static) load is moved around the structure.

Two examples of influence lines are given in Figure 5.8. Figure 5.8(a) shows the influ-

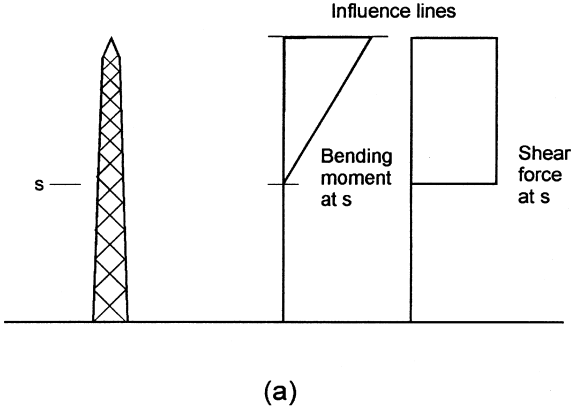

Figure 5.8 Examples of influence lines for an arch roof and a tower.

ence lines for the bending moment and shear force at a level, s, halfway up a lattice tower. These are relatively simple functions; in the case of the shear force loads (or wind pressures) above the level s have uniform effect on the shear force at that level. The influence line for the bending moment varies linearly from unity at the top to zero at the level s; thus wind pressures at the top of the structure have a much larger effect than those lower down, on the bending moment, which, in turn, is closely related to the axial forces in the leg members of the tower. It should be noted that loads or wind pressures below the level s have *no* effect on the shear force or bending moment at that level.

Figure 5.8(b) shows the influence line for the bending moment at a point in an arch roof. In this case, the sign of the influence line changes along the arch. Thus wind pressures applied in the same direction at different parts of the roof may have opposite effects on the bending moment at C, M_c.

It is important to take into account these non-uniform influences when considering the structural effects of wind loads, even for apparently simple structures, especially for the fluctuating part of the loading.

5.3.6 Along-wind response of a structure with distributed mass – modal analysis

The usual approach to the calculation of the dynamic response of multi-degree-of-freedom structures to dynamic forces, including resonance effects, is to expand the complete displacement response as a summation of components associated with each of the natural modes of vibration:

$$x(z,t) = \Sigma a_j(t)\phi_j(z) \tag{5.16}$$

where j denotes the natural modes; z is a spatial coordinate on the structure; a_j (t) is a time-varying modal (or generalized) coordinate; and ϕ_j (z) is a mode shape for the jth mode.

Modal analysis is discussed in most texts on structural dynamics (e.g. Clough and Penzien (1975), Warburton (1976)).

The approach will be described here in the context of a two-dimensional or 'line-like' structure, with a single spatial coordinate, z, but it can easily be extended to more complex geometries.

Equation (5.16) can be used to determine the complete response of a structure to random forcing, i.e. including the mean component, $\bar{x}$, and the subresonant (background) fluctuating component, as well as the resonant responses.

The result of this approach is that separate equations of motion can be written for the modal coordinate $a_j(t)$, for each mode of the structure:

$$G_j\ddot{a} + C_j\dot{a} + K_j a = Q_j(t) \tag{5.17}$$

where G_j is the generalized mass equal to $\int_0^L m(z)\phi_j^2(z)dz$, $m(z)$ is the mass per unit length along the structure, L is the length of the structure, C_j is the modal damping $(=2\eta_j G_j \omega_j)$, K_j is the modal stiffness, η_j is the damping as a fraction of critical for the jth mode, ω_j is the natural undamped circular frequency for the jth mode $\left(=2\pi n_j = \sqrt{\frac{K_j}{G_j}}\right)$, $Q_j(t)$ is the

generalized force, equal to $\int_0^L f(z,t)\phi_j(z)dz$ and $f(z,t)$ is the force per unit length along the structure.

$f(z,t)$ can be taken as along-wind or cross-wind forces. For along-wind forces, applying a 'strip' assumption, which relates the forces on a section of the structure with the flow conditions upstream of the section, it can be written as:

$$f(z,t) = C_d(z).b(z)\frac{1}{2}\rho_a U^2(z,t) \tag{5.18}$$

where $C_d(z)$ is a local drag coefficient, $b(z)$ is the local breadth and $U(z,t)$ is the longitudinal velocity upstream of the section. If the structure is moving, this should be a relative velocity, which then generates an aerodynamic damping force (Section 5.5.1 and Holmes (1996a)). However, at this point we will assume the structure is stationary, in which case $U(z,t)$ can be written:

$$U(z,t) = \bar{U}(z) + u'(z,t)$$

where $u'(z,t)$ is the fluctuating component of longitudinal velocity (zero mean).

Then from equation (5.18),

$$f(z,t) = C_d(z).b(z)\rho_a\left[\frac{1}{2}\bar{U}^2(z) + \bar{U}(z)u'(z,t) + \frac{1}{2}u'^2(z,t)\right]$$

Neglecting the third term within the square brackets, the fluctuating sectional along-wind force is given by:

$$f'(z,t) = C_d(z).b(z)\rho_a\bar{U}(z)u'(z,t)$$

and the instantaneous fluctuating generalized force is therefore:

$$Q'_j(t) = \int_0^L f'(z,t)\phi_j(z)dz = \int_0^L C_d(z).b(z)\rho_a\bar{U}(z)u'(z,t)\phi_j(z)dz$$

Applying the same procedure used in Section 4.6.6, the mean square generalized force is:

$$\overline{Q'^2} = \int_0^L\int_0^L \overline{f'(z_1)f'(z_2)}\phi_j(z_1)\phi_j(z_2)dz_1dz_2$$

$$= \rho_a{}^2\int_0^L\int_0^L \overline{u'(z_1)u'(z_2)}C_d(z_1).C_d(z_2)b(z_1)b(z_2)\bar{U}(z_1)\bar{U}(z_2)\phi_j(z_1)\phi_j(z_2)dz_1dz_2$$

This can be simplified for a uniform cross-section, with $C_D(z)$ and $b(z)$ constant with z:

$$\overline{Q'^2} = (\rho_a C_d b)^2 \int_0^L \int_0^L \overline{u'(z_1)u'(z_2)}\bar{U}(z_1)\bar{U}(z_2)\phi_j(z_1)\phi_j(z_2)dz_1dz_2 \tag{5.19}$$

where $\overline{u'(z_1)u'(z_2)}$ is the covariance for the fluctuating velocities at heights z_1 and z_2. If the standard deviation of velocity fluctuations is constant with z, then the covariance can be written:

$$\overline{u'(z_1)u'(z_2)} = \sigma_u^2 \rho_{uu}(z_1,z_2)$$

where $\rho_{uu}(z_1,z_2)$ is the correlation coefficient for fluctuating velocities at heights z_1 and z_2, defined in Section 3.3.5.

The spectral density of $Q'_j(t)$ can be obtained in analogous way to the mean square value:

$$S_{Qj}(n) = (\rho C_d b)^2 \int_0^L \int_0^L Co(z_1,z_2,n)\bar{U}(z_1)\bar{U}(z_2)\phi_j(z_1)\phi_j(z_2)dz_1dz_2 \tag{5.20}$$

where $Co(z_1,z_2,n)$ is the co-spectral density of the longitudinal velocity fluctuations (Section 3.3.6), (defined in random process theory, e.g. Bendat and Piersol (1999)).

Analogously with equation (5.6), the spectral density of the modal coordinate $a_j(t)$ is given by:

$$S_{aj}(n) = \frac{1}{K_j^2}|H_j(n)|^2 S_{Qj}(n) \tag{5.21}$$

where the mechanical admittance for the jth mode is:

$$|H_j(n)|^2 = \frac{1}{\left[1-\left(\frac{n}{n_j}\right)^2\right]^2 + 4\eta_j^2\left(\frac{n}{n_j}\right)^2} \tag{5.22}$$

The mean square value of $a_j(t)$ can then be obtained by integration of equation (5.21) with respect to frequency:

$$\overline{a_j'^2} = \int_0^\infty S_{aj}(n).dn$$

Applying equation (5.16), the mean square displacement is obtained from:

$$\overline{x'^2} = \sum_{j=1}^{N}\sum_{k=1}^{N} \overline{a_j'a_k'}\phi_j(z)\phi_k(z)$$

If cross-coupling between modes can be neglected (however, see Section 5.3.7), the above equation becomes:

$$\overline{x'^2} = \sum_{j=1}^{N} \overline{a_j'^2}\phi_j^2(z) \tag{5.23}$$

The mean square value of any other response, r, (e.g. bending moment, stress) can similarly be obtained if the response, R_j for a unit value of the modal coordinate, a_j, is known. That is:

$$\overline{r'^2} = \sum_{j=1}^{N} \overline{a_j'^2}R_j^2 \tag{5.24}$$

5.3.7 Along-wind response of a structure with distributed mass – separation of background and resonant components

In the case of wind loading, the method described in the previous section is not an efficient one. For the vast majority of structures, the natural frequencies are at the high end of the range of forcing frequencies from wind loading. Thus the resonant components as j increases in equation (5.16) become very small. However, the contributions to the mean and background fluctuating components for j greater than 1 in equation (5.16) *may not be small.* Thus it is necessary to include higher modes ($j>1$) in equation (5.16) not for their resonant contributions, but to accurately determine the mean and background contributions. For example, Vickery (1995) found that over twenty modes were required to determine the mean value of a response, and over ten values were need to compute the variance. Also for the background response, cross coupling of modes cannot be neglected, i.e. equation (5.23) is not valid.

A much more efficient approach is to separately compute the mean and background components, as for a quasi-static structure. Thus the total peak response, $\hat{r}$, can be taken to be:

$$\hat{r} = \bar{r} + \sqrt{\hat{r}_B^2 + \sum_j (\hat{r}_{R,j}^2)} \tag{5.25}$$

where $\hat{r}_B$ is the peak background response equal to $g_B\sigma_B$; and $\hat{r}_{R,j}$ is the peak resonant response computed for the jth mode, equal to $g_j\sigma_R$,j. This approach is illustrated in Figure 5.1.

g_B and g_j are peak factors which can be determined from equation (5.15); in the case of the resonant response, the cycling rate, ν, in equation (5.15), can be taken as the natural frequency, n_j.

The mean square value of the quasi-static fluctuating (background) value of any reponse, r, is:

$$\overline{r_B'^2} = \sigma_B{}^2 = \int_0^L \int_0^L \overline{f'(z_1)f'(z_2)} I_r(z_1) I_r(z_2) dz_1 dz_2 =$$

$$\rho_a^2 \int_0^L \int_0^L \overline{u'(z_1)u'(z_2)} C_d(z_1).C_d(z_2) b(z_1) b(z_2) \bar{U}(z_1) \bar{U}(z_2) I_r(z_1) I_r(z_2) dz_1 dz_2 \quad (5.26)$$

where $I_r(z)$ is the influence line for r, i.e. the value of r when a unit load is applied at z.

The resonant component of the response in mode j, can be written, to a good approximation, as:

$$\overline{r_{Rj}'^2} = \frac{S_{Qj}(n_j) R_j^2}{K_j^2} \int_0^\infty |H_j(n)|^2 .dn = \frac{\pi n_1 . S_{Qj}(n_j) R_j^2}{4\eta_j K_j^2} \quad (5.27)$$

since the integral $\int_0^\infty |H_j(n)|^2 .dn$, evaluated by the method of poles (Crandall and Mark, 1963), is equal to $(\pi n_j / 4\eta_j)$.

5.4 Effective static loading distributions

5.4.1 Introduction

Effective static wind load distributions are those loadings that produce the correct expected values of peak load effects, such as bending moments, axial forces in members, or deflections, generated by the fluctuating wind loading. The effective peak loading distributions associated with the mean wind loading, the fluctuating quasi-static or background response and the resonant response are identified, and combined to give a total effective peak wind loading distribution.

Following the procedure described in the previous sections, effective static peak loading distributions can be separately derived for the following three components:

- mean component
- background or sub-resonant component and
- resonant components.

The background component is derived making use of a formula derived by Kasperski and Niemann (1992), and depends on the load effect in question. The resonant component comprises an inertial loading, similar to that used in earthquake engineering.

The approach will be illustrated by examples of buildings with long-span roofs and freestanding lattice towers and chimneys. Simplifications will be suggested to make the method more palatable to structural engineers used to analysing and designing with static loadings.

The main advantage of the effective static load distribution approach is that the distributions can be applied to static structural analysis computer programs for use in detail structural design. The approach can be applied to any type of structure (Holmes and Kasperski, 1996).

5.4.2 Mean load distributions

The mean wind loading on a structure which does not distort the airflow significantly can be obtained simply by relating the mean local pressure or force per unit length to the mean wind speed. Thus for the mean along-wind force per unit height acting on a tower:

$$\bar{f}(z) = [0.5\rho_a \bar{U}(z)^2] C_d b(z) \tag{5.28}$$

where ρ_a is the density of air; $\bar{U}(z)$ is the mean wind speed at height z; C_d is a drag coefficient; and $b(z)$ is the reference breadth at the height z.

The mean value of any load effect (e.g. shear force, bending moment, deflection) can be obtained by integrating the local load with the influence line over the appropriate height. However, if the purpose is to derive an equivalent static loading, then equation (5.28) is already in this form.

In the case of 'solid' structures (such as cooling towers and most buildings) with at least two dimensions comparable to the size of turbulent eddies in the atmosphere, equation (5.28) cannot be used, but wind-tunnel tests can be employed to determine mean pressure coefficients, $\bar{C}_p$, which can then be used with a reference wind speed, $\bar{U}_h$, to determine local mean pressures on the structure:

$$\bar{p}(z) = [0.5\rho_a \bar{U}_h^2] \bar{C}_p \tag{5.29}$$

5.4.3 Background loading distributions

As discussed previously, the background wind loading is the quasi-static loading produced by fluctuations due to turbulence, but with frequencies too low to excite any resonant response. Over the duration of a windstorm, because of the incomplete correlations of pressures at various points on a structure, loadings varying both in space and time will be experienced. It is necessary to identify those instantaneous loadings which produce the critical load effects in a structure. The formula which enables this to be done is the 'Load–Response Correlation' formula derived by Kasperski and Niemann (1992).

This formula gives the expected 'instantaneous' pressure distribution associated with the maximum or minimum load effect. Thus for the maximum value, $\hat{r}$, of a load effect, r:

$$(p_i)_{\hat{r}} = \bar{p}_i + g_B . \rho_{r,pi} . \sigma_{pi} \tag{5.30}$$

where $\bar{p}_i$ and σ_{pi} are the mean and root-mean-square (r.m.s.) pressures at point or panel, i.

$\rho_{r,pi}$ is the correlation coefficient between the fluctuating load effect, and the fluctuating pressure at point i (this can be determined from the correlation coefficients for the fluctuating pressures at all points on the tributary area, and from the influence coefficients); and g_B is the peak factor for the background response which normally lies in the range 2.5 to 5.

A simple example of the application of this formula is given in Appendix F.

The second term on the right-hand side of equation (5.30) represents the background fluctuating load distribution. This term can also be written in the form of a continuous distribution:

$$f_B(z) = g_B \rho(z) \sigma_p(z) \tag{5.31}$$

where $\rho(z)$ denotes the correlation coefficient between the fluctuating load at position z

on the structure, and the load effect of interest; and $\sigma_p(z)$ is the r.m.s. fluctuating load at position z.

In equation (5.30), the correlation coefficient, $\rho_{r,pi}$, can be shown to be given by:

$$\rho_{r,pi} = \sum_k [\overline{p_i(t)p_k(t)}I_k]/(\sigma_{pi}\sigma_r) \tag{5.32}$$

where I_k is the influence coefficient for a pressure applied at position, k.

The standard deviation of the structural load effect, σ_r, is given by (Holmes and Best, 1981):

$$\sigma_r^2 = \sum_i \sum_k \overline{p_i(t)p_k(t)}\, I_i I_k \tag{5.33}$$

When the continuous form is used, equations (5.32) and (5.33) are replaced by an integral form (Holmes, 1996b):

$$\rho(z) = \frac{\int_s^h \overline{f'(z)f'(z_1)} I_r(z_1) b(z_1) dz_1}{\left\{ \int_s^h \int_s^h \overline{f'(z_1)f'(z_2)} I_r(z_1) I_r(z_2) b(z_1) b(z_2) dz_1 dz_2 \right\}^{\frac{1}{2}} \sqrt{\overline{f'^2(z)}}} \tag{5.34}$$

where $I_r(z)$ now denotes the influence function for the load effect, r, as a function of position z, and $b(z)$ is the breadth of the structure at position z. For a vertical structure, the integrations in equation (5.34) are carried out for the height range from s, the height at which the load effect (e.g. bending moment, shearing force, member force) is being evaluated, and the top of the structure, h.

Clearly, since the correlation coefficient, $\rho_{r,pi}$, calculated by equation (5.32), or $\rho(z)$ calculated by equation (5.34), are dependent on the particular load effect, then the background load distribution will also depend on the nature of the load effect.

Figures 5.9 and 5.10 give examples of background loading distributions calculated using these methods. Figure 5.9 shows examples of peak load (mean + background) distributions for a support reaction (dashed) and a bending moment (dotted) in an arch roof. These distributions fall within an envelope formed by the maximum and minimum pressure distributions along the arch. It should also be noted that the distribution for the bending moment at C includes a region of positive pressure.

Figure 5.10 shows the background pressure distribution for the base shear force and base bending moment on a lattice tower 160 m high, determined by calculation using equation (5.23), (Holmes, 1996b). The maxima for these distributions occur at around 70 m height for the base shear and about 120 m for the base bending moment. An approximation (Holmes, 1996b) to these distributions, which is independent of the load effect but dependent on the height at which the load effect is evaluated, is also shown in Figure 5.10.

5.4.4 Load distributions for resonant response (single resonant mode)

The equivalent load distribution for the resonant response in the first mode can be represented as a distribution of inertial forces over the length of the structure. Thus, an equivalent load distribution for the resonant response, $f_R(z)$, is given by:

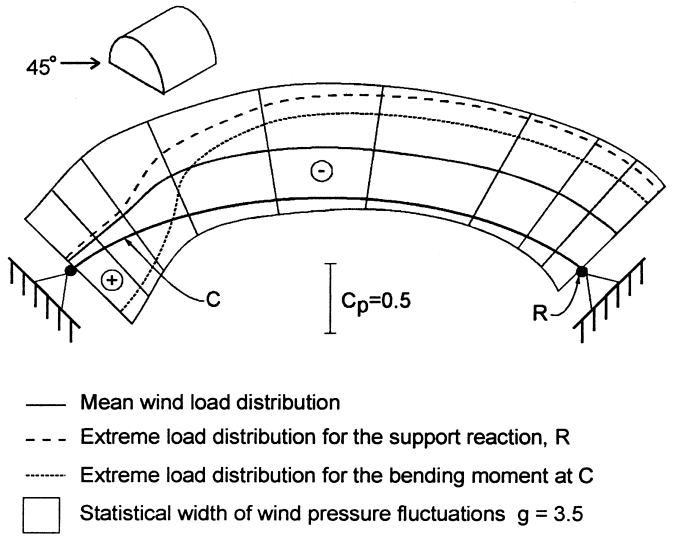

Figure 5.9 Mean and effective background load distributions for an arch roof (after Kasperski and Niemann, 1992.

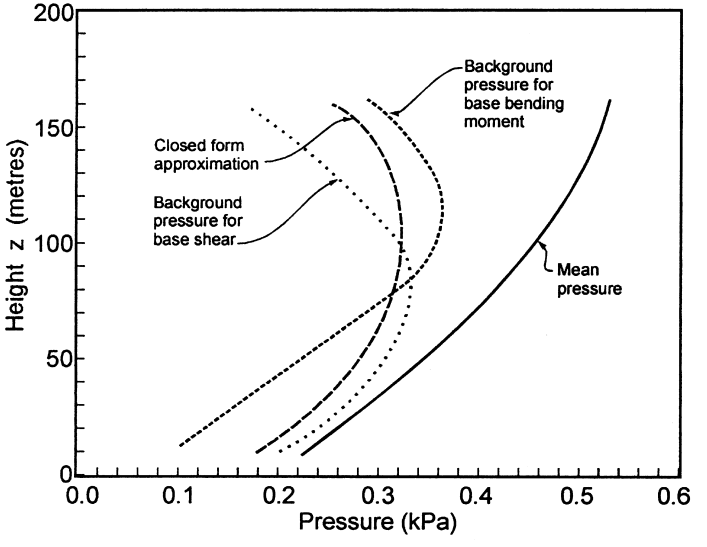

Figure 5.10 Mean and effective background load distributions for a 160 metre tower (after Holmes, 1996b).

$$f_R(z) = g_R m(z)(2\pi n_1)^2 \sqrt{\overline{a'^2}}\phi_1(z) \tag{5.35}$$

where g_R is the peak factor for resonant response; $m(z)$ is a mass per unit length; n_1 is the first mode natural frequency; $\sqrt{\overline{a'^2}}$ is the r.m.s. modal coordinate (resonant contribution only), and $\phi_1(z)$ is the mode shape for the first mode of vibration.

Determination of the r.m.s. modal coordinate requires knowledge of the spectral density of the exciting forces, the correlation of those forces at the natural frequency (or aerodynamic admittance), and the modal damping and stiffness, as discussed in Sections 5.3.4 and 5.3.5.

5.4.5 Combined load distribution

The combined effective static load distribution for mean, background and resonant components (one mode) is obtained as follows:

$$f_c(z) = \bar{f}(z) + W_{back} f_B(z) + W_{res}(z) f_R(z) \tag{5.36}$$

where the absolute values of the weighting factors W_{back} and W_{res} are given by:

$$|W_{back}| = \frac{g_B \sigma_{r,B}}{(g_B{}^2 \sigma_{r,B}{}^2 + g_R{}^2 \sigma_{r,R}{}^2)^{1/2}} \quad |W_{res}| = \frac{g_R \sigma_{r,R}}{(g_B{}^2 \sigma_{r,B}{}^2 + g_R{}^2 \sigma_{r,R}{}^2)^{1/2}} \tag{5.37}$$

The above assumes that the fluctuating background and resonant components are uncorrelated with each other, so that equation (5.25) applies. W_{back} and W_{res}will be positive if the influence line of the load effect, r, and the mode shape are both all positive, but either could be negative in many cases.

By multiplying by the influence coefficient and summing over the whole structure, equations (5.36) will give equation (5.25) for the total peak load effect.

An alternative to equation (5.36) is to combine the background and resonant distributions in the same way that the load effects themselves were combined (equation (5.25)), i.e.:

$$f_c(z) = \bar{f}(z) + \sqrt{[f_B(z)]^2 + [f_R(z)]^2} \tag{5.38}$$

The second term on the right-hand-side is an approximation, to the correct combination formula (equation 5.36), and is independent of the load effect or its influence line. equation (5.38) with positive and negative signs taken in front of the square root is, in fact an 'envelope' of the combined distributions for all load effects. However it is a good approximation for cases where the influence line $I_r(z)$, and the mode shape have the same sign for all z, (Holmes, 1996b).

Examples of the combined distribution, calculated using equation (5.38), are given in Figure 5.11 for a 160 m lattice tower (Holmes, 1996b). When the resonant component is included, the combined loading can exceed the 'peak gust pressure envelope', i.e. the expected limit of non-simultaneous peak pressures, as is the case in Figure 5.11 for the bending moment at 120 m.

Equations (5.36) and (5.37) can be extended to cover more than one resonant mode by introducing an additional term for each participating mode of vibration. An example of combined equivalent static load distributions, when more than one resonant mode contributes significantly, is discussed in Section 12.3.4.

5.5 Aeroelastic forces

For very flexible, dynamically wind-sensitive structures, the motion of the structure may itself generate aerodynamic forces. In extreme cases, the forces may be of such a magni-

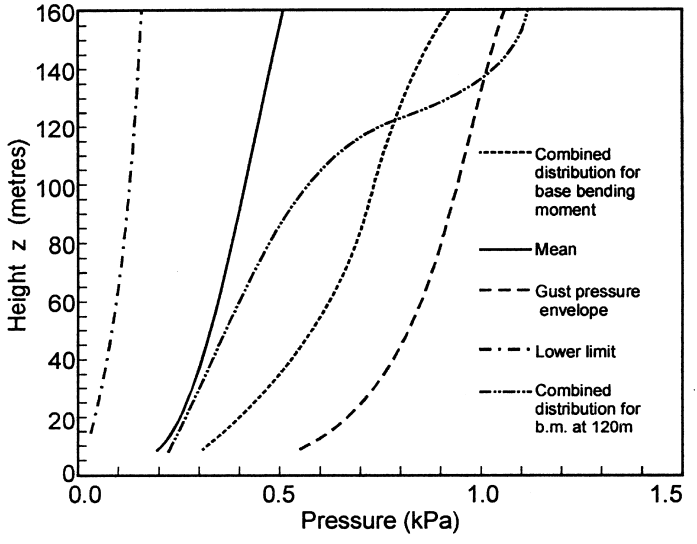

Figure 5.11 Mean and combined (including resonant contributions) load distributions for a 160 metre tower (Holmes, 1996b).

tude and act in a direction to sustain or increase the motion; in these cases an unstable situation may arise such that a small disturbance may initiate a growing amplitude of vibration. This is known as 'aerodynamic instability' – examples of which are the 'galloping' of iced-up transmission lines and the flutter of long suspension bridges (such as the Tacoma Narrows Bridge failure of 1940).

On the other hand 'aerodynamic damping' forces may act to reduce the amplitude of vibration induced by wind. This is the case with the along-wind vibration of tall structures, such as lattice towers of relatively low mass.

The subject of aeroelasticity and aerodynamic stability is a complex one, and one which most engineers will not need to be involved with. However, some discussion of the principles will be given in this section. A number of general reviews are available of this aspect of wind loads (e.g. Scanlan, 1982).

5.5.1 Aerodynamic damping

Consider the along-wind motion of a structure with a square cross-section, as shown in Figure 5.12. Ignoring initially the effects of turbulence, we will consider only the mean wind speed, $\bar{U}$. If the body itself is moving in the along-wind direction with a velocity, $\dot{x}$, the relative velocity of the air with respect to the moving body is $(\bar{U}-\dot{x})$. We then have a drag force per unit length of the structure equal to:

$$D = C_D \frac{1}{2}\rho_a b(\bar{U} - \dot{x})^2 \cong C_D \frac{1}{2}\rho_a b\bar{U}^2\left(1 - \frac{2\dot{x}}{\bar{U}}\right)$$

$$= C_D \frac{1}{2}\rho_a b\bar{U}^2 - C_D \rho_a b\bar{U}\dot{x}$$

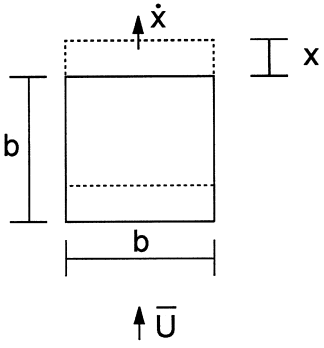

Figure 5.12 Along-wind relative motion and aerodynamic damping.

for small values of $\dot{x}/\bar{U}$. The second term on the right-hand-side is a quantity proportional to the structure velocity, $\dot{x}$, and this represents a form of damping. When transferred to the left-hand-side of the equation of motion (equation 5.2), it combines with the structural damping term, $c\dot{x}$, to reduce the aerodynamic response.

For a continuous structure, the along-wind aerodynamic damping coefficient in mode j can be shown to be (Holmes, 1996a):

$$C_{aero,j} = \rho_a \int_0^L C_d(z) b(z) \bar{U}(z) \phi_j^2(z) dz$$

giving a critical aerodynamic damping ratio, $\eta_{aero,j}$, equal

$$\eta_{aero,j} = \frac{\rho_a \int_0^L C_d(z) b(z) \bar{U}(z) \phi_j^2(z) dz}{4\pi n_j G_j} \tag{5.39}$$

5.5.2 Galloping

Galloping is a form of single-degree-of-freedom aerodynamic instability, which can occur for long bodies with certain cross-sections. It is a pure translational, cross-wind vibration. Consider a section of a body with a square cross-section as shown in Figure 5.13.

The aerodynamic force per unit length, in the z-direction, is obtained from the lift and drag by a change of axes (Figure 4.3).

$$F_z = D \sin\alpha + L \cos\alpha = \frac{1}{2}\rho_a \bar{U}^2 b (C_D \sin\alpha + C_L \cos\alpha)$$

Hence,

$$\frac{dF_z}{d\alpha} = \frac{1}{2}\rho_a \bar{U}^2 b \left(C_D \cos\alpha + \frac{dC_D}{d\alpha}\sin\alpha - C_L \sin\alpha + \frac{dC_L}{d\alpha}\cos\alpha\right)$$

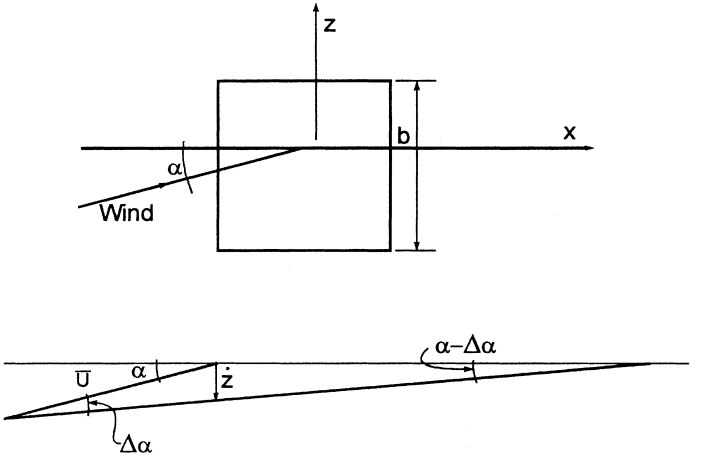

Figure 5.13 Cross-wind relative motion and galloping.

Setting α equal to zero (for flow in the x-direction),

$$\frac{dF_z}{d\alpha} = \frac{1}{2}\rho_a \bar{U}^2 b\left(C_D + \frac{dC_L}{d\alpha}\right) \tag{5.40}$$

If the body is moving in the z direction with velocity, $\dot{z}$, there will be a reduction in the apparent angle of attack of the flow by $\dot{z}/\bar{U}$, or an increase in angle of attack by $-\dot{z}/\bar{U}$.

From equation (5.40),

$$\Delta F_z \cong \frac{1}{2}\rho_a \bar{U}^2 b\left(C_D + \frac{dC_L}{d\alpha}\right)\Delta\alpha$$

Substituting, $\Delta\alpha = -\dot{z}/\bar{U}$,

$$\Delta F_z \cong \frac{1}{2}\rho_a \bar{U}^2 b\left(C_D + \frac{dC_L}{d\alpha}\right)\left(-\frac{\dot{z}}{\bar{U}}\right) = -\frac{1}{2}\rho_a \bar{U} b\left(C_D + \frac{dC_L}{d\alpha}\right)\dot{z} \tag{5.41}$$

If $\left(C_D + \dfrac{dC_L}{d\alpha}\right) < 0$, there will be an aerodynamic force in the z direction, proportional to the velocity of the motion, $\dot{z}$, or a *negative* aerodynamic damping term when it is transposed to the left-hand-side of the equation of motion. This is known as 'den Hartog's criterion'.

This situation can arise for a square section, which has a negative slope $\dfrac{dC_L}{d\alpha}$, with a magnitude greater than C_D, for α equal to zero (Figure 5.13).

5.5.3 *Flutter*

Consider now a two-dimensional bluff body able to move, with elastic restraint, in both vertical translation and rotation (i.e. bending and torsion deflections).

The body shown in Figure 5.14 is being twisted, and the section shown is rotating with an angular velocity, $\dot{\theta}$, radians per second. This gives the relative wind, with respect to the rotating body, a vertical component of velocity at the leading edge of $\dot{\theta}d/2$, and hence a relative angle of attack between the apparent wind direction and the rotating body of $-\dot{\theta}d/2\bar{U}$. This effective angle of attack can generate both a vertical force, and a moment if the centre of pressure is not collinear with the centre of rotation of the body. These aeroelastic forces can generate instabilities, if they are not completely opposed by the structural damping in the rotational mode. Aerodynamic instabilities involving rotation are known as 'flutter', using aeronautical parlance, and are a potential problem with the suspended decks of long-span bridges.

The equations of motion (per unit mass or moment of inertia) for the two degrees-of freedom of a bluff body can be written (Scanlan and Tomko, 1971; Scanlan and Gade, 1977; Matsumoto, 1996):

$$\ddot{z} + 2\eta_z\omega_z\dot{z} + \omega_z^2 z = \frac{F_z(t)}{m} + H_1\dot{z} + H_2\dot{\theta} + H_3\theta \tag{5.42}$$

$$\ddot{\theta} + 2\eta_\theta\omega_\theta\dot{\theta} + \omega_\theta^2\theta = \frac{M(t)}{I} + A_1\dot{z} + A_2\dot{\theta} + A_3\theta \tag{5.43}$$

The terms A_i, and H_i are linear aeroelastic coefficients, or *flutter derivatives*, which are usually determined experimentally for particular cross-sections. They are functions of non-dimensional or *reduced* frequency. $F_z(t)$ and $M(t)$ are forces and moments due to other mechanisms which act on a static body (e.g. turbulent buffeting or vortex shedding). ω_z ($=2\pi n_z$), and ω_θ ($=2\pi n_\theta$) are the undamped circular frequencies in still air for vertical motion and rotation, respectively.

Note that equations (5.42) and (5.43) have been 'linearised', i.e. they only contain terms in $\dot{z}$, θ, $\dot{\theta}$, etc. There could be smaller terms in $\dot{z}^2$, θ^2, $\dot{\theta}^3$, etc. The two equations are 'coupled' second-order linear differential equations. The coupling arises from the ocurrence of terms in z and θ, or their derivatives in both equations. This can result in coupled aeroelastic instabilities, which are a combination of vertical (bending) and rotational (torsion) motions, depending on the signs and magnitudes of the A_i and H_I derivatives. All bridge decks will reach this state at a high enough wind speed.

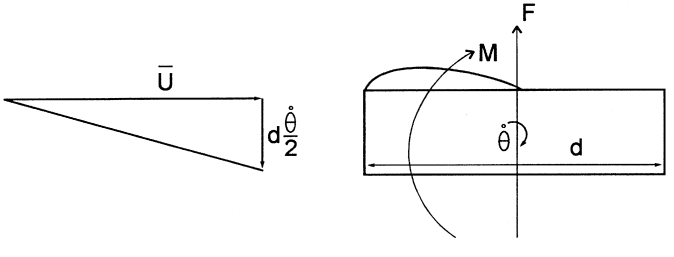

Figure 5.14 Aeroelastic forces generated by rotation of a cross section.

Several particular types of instability for bluff bodies have been defined. Three of these are summarized in Table 5.1.

Coupled aeroelastic instabilities in relation to long-span bridge decks, and flutter derivatives, are further discussed in Chapter 12, Bridges.

5.5.4 Lock-in

Motion-induced forces can occur during vibration produced by vortex shedding (Section 4.6.3). Through a feedback mechanism, the frequency of the shedding of vortices can 'lock-in' to the frequency of motion of the body. The strength of the vortices shed, and the fluctuating forces resulting are also enhanced. *Lock-in* has been observed many times during the vibration of lightly damped cylindrical structures such as steel chimneys, and occasionally during the vortex-induced vibration of long-span bridges.

5.6 Fatigue under wind loading

5.6.1 Metallic fatigue

The 'fatigue' of metallic materials under cyclic loading has been well researched, although the treatment of fatigue damage under the random dynamic loading characteristic of wind loading is less well developed.

In the usual failure model for the fatigue of metals it is assumed that each cycle of a sinusoidal stress response inflicts an increment of damage which depends on the amplitude of the stress. Each successive cycle then generates additional damage which accumulates in proportion to the number of cycles until failure occurs. The results of constant amplitude fatigue tests are usually expressed in the form of an *s-N* curve, where s is the stress amplitude, and N is the number of cycles until failure. For many materials, the *s-N* curve is well approximated by a straight line when log s is plotted against log N (Figure 5.15). This implies an equation of the form:

$$Ns^m = K \tag{5.44}$$

where K is a constant which depends on the material, and the exponent m varies between about 5 and 20.

A criterion for failure under repeated loading, with a range of different amplitudes is Miner's rule:

$$\sum\left(\frac{n_i}{N_i}\right) = 1 \tag{5.45}$$

Table 5.1 Types of aerodynamic instabilities

Name	*Conditions*	*Type of motion*	*Type of section*
Galloping	$H_1>0$	translational	Square section
'Stall' flutter	$A_2>0$	rotational	Rectangle, H-section
'Classical' flutter	$H_2>0$, $A_1>0$	coupled	Flat plate, airfoil

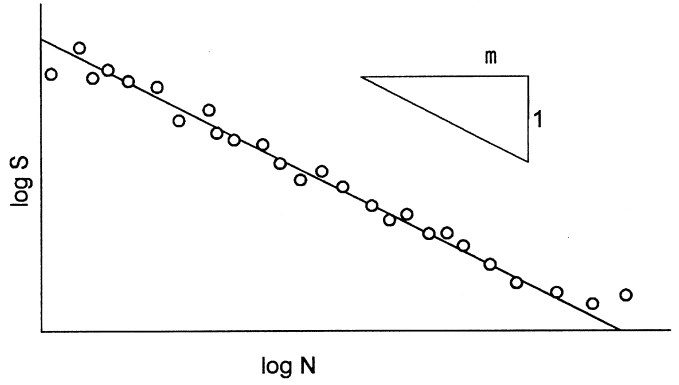

Figure 5.15 Form of a typical *s-N* curve.

where n_i is the number of stress cycles at an amplitude for which N_i cycles are required to cause failure. Thus failure is expected when the sum of the fractional damage for all stress levels is unity.

Note that there is no restriction on the *order* in which the various stress amplitudes are applied in Miner's rule. Thus we may apply it to a random loading process which can be considered as a series of cycles with randomly varying amplitudes.

5.6.2 Narrow band fatigue loading

Some wind loading situations produce resonant 'narrow-band' vibrations. For example, the along-wind response of structures with low natural frequencies (Section 5.3.1), and cross-wind vortex induced response of circular cylindrical structures with low damping. In these cases, the resulting stress variations can be regarded as quasi-sinusoidal with randomly varying amplitudes, as shown in Figure 5.16.

For a narrow-band random stress $s(t)$, the proportion of cycles with amplitudes in the range from s to $s + \delta s$, is $f_p(s)$. δs, where $f_p(s)$ is the probability density of the peaks. The total number of cycles in a time period, T, is $\nu_o^+ T$, where ν_o^+ is the rate of crossing of the

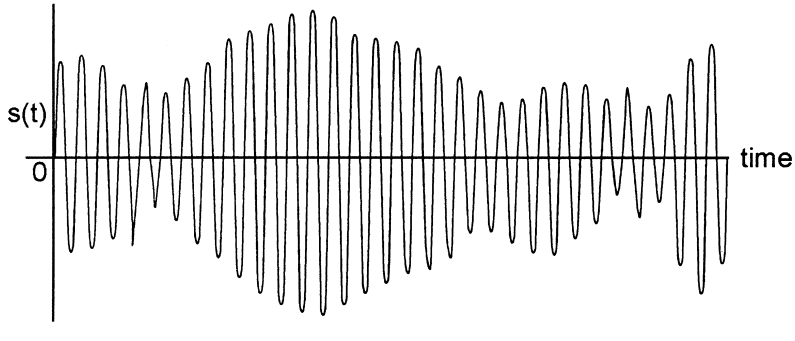

Figure 5.16 Stress-time history under narrow-band random vibrations.

mean stress. For narrow band resonant vibration, ν_o^+ may be taken to be equal to the natural frequency of vibration.

Then the total number of cycles with amplitudes in the range s to δs,

$$n(s) = \nu_o^+ T f_p(s).\delta s \tag{5.46}$$

If $N(s)$ is the number of cycles at amplitude s to cause failure, then the fractional damage at this stress level

$$= \frac{n(s)}{N(s)} = \frac{\nu_o^+ T f_p(s) s^m \delta s}{K}$$

where equation (5.46) has been used for $n(s)$, and equation (5.44) for $N(s)$.

The total expected fractional damage over all stress amplitudes is then, by Miner's rule:

$$D = \sum_0^\infty \frac{n(s)}{N(s)} = \frac{\nu_o^+ T \int_0^\infty f_p(s) s^m ds}{K} \tag{5.47}$$

Wind-induced narrow-band vibrations can be taken to have a normal or Gaussian probability distribution (Section C3.1, Appendix C). If this is the case then the peaks or amplitudes, s, have a Rayleigh distribution (e.g. Crandall and Mark, 1963):

$$f_p(s) = \frac{s}{\sigma^2} \exp\left(- \frac{s^2}{2\sigma^2} \right) \tag{5.48}$$

where σ is the standard deviation of the entire stress history. Derivation of equation (5.48) is based on the level crossing formula of Rice (1944–5).

Substituting into equation (5.47),

$$D = \frac{\nu_o^+ T}{K\sigma^2} \int_0^\infty s^{m+1} \exp\left(- \frac{s^2}{2\sigma^2} \right) ds = \frac{\nu_o^+ T}{K} (\sqrt{2}\sigma)^m \Gamma\left(\frac{m}{2} + 1 \right) \tag{5.49}$$

Here the following mathematical result has been used (Crandall and Mark, 1963):

$$\int_0^\infty x^n \exp\left(- \frac{x^2}{2\sigma^2} \right) dx = \frac{(\sqrt{2}\sigma)^{n+1}}{2} \Gamma\left(\frac{n+1}{2} \right) \tag{5.50}$$

$\Gamma(x)$ is the Gamma function.

Equation (5.49) is a very useful 'closed-form' result, but it is restricted by two important assumptions:

- 'high-cycle' fatigue behaviour in which steel is in the elastic range, and for which an s-N curve of the form of equation (5.44) is valid, has been assumed

- narrow band vibration in a single resonant mode of the form shown in Figure 5.16 has been assumed. In wind loading this is a good model of the behaviour for vortex-shedding induced vibrations in low turbulence conditions. For along-wind loading, the background (subresonant) components are almost always important and result in a random wide-band response of the structure.

5.6.3 Wide band fatigue loading

Wide band random vibration consists of contributions over a broad range of frequencies, with a large resonant peak – this type of response is typical for wind loading (Figure 5.7). A number of cycle counting methods for wide band stress variations have been proposed (Dowling, 1972). One of the most realistic of these is the 'rainflow' method proposed by Matsuishi and Endo (1968). In this method, which uses the analogy of rain flowing over the undulations of a roof, cycles associated with complete hysteresis cycles of the metal, are identified. Use of this method rather than a simple level-crossing approach which is the basis of the narrow-band approach described in Section 5.6.2, invariably results in fewer cycle counts.

A useful empirical approach has been proposed by Wirsching and Light (1980). They proposed that the fractional fatigue damage under a wide-band random stress variation can be written as:

$$D = \lambda D_{nb} \tag{5.51}$$

where, D_{nb} is the damage calculated for narrow-band vibration with the same standard deviation, σ (equation 5.49). λ is a parameter determined empirically. The approach used to determine λ was to use simulations of wide-band processes with spectral densities of various shapes and bandwidths, and rainflow counting for fatigue cycles.

The formula proposed by Wirsching and Light to estimate λ was:

$$\lambda = a + (1 - a)(1 - \varepsilon)^b \tag{5.52}$$

where a and b are functions of the exponent m (equation 5.44), obtained by least-squares fitting, as follows:

$$a \cong 0.926 - 0.033\ \mathrm{m} \tag{5.53}$$

$$b \cong 1.587\ \mathrm{m} - 2.323 \tag{5.54}$$

ε is a spectral bandwidth parameter equal to:

$$\varepsilon = 1 - \frac{\mu_2^2}{\mu_0 \mu_4} \tag{5.55}$$

where, μ_k is the kth moment of the spectral density defined by:

$$\mu_k = \int_0^\infty n^k S(n) dn \tag{5.56}$$

For narrow band vibration ε tends to zero, and, from equation (5.52), λ approaches 1. As ε tends to its maximum possible value of 1, λ approaches *a*, given by equation (5.53). These values enable upper and lower limits on the damage to be determined.

5.6.4 Effect of varying wind speed

Equation (5.49) applies to a particular standard deviation of stress, σ, which in turn is a function of mean wind speed, $\bar{U}$ This relationship can be written in the form:

$$\sigma = A\bar{U}^n \tag{5.57}$$

The mean wind speed, $\bar{U}$, itself, is a random variable. Its probability distribution can be represented by a Weibull distribution (see Section 2.5 and C.3.4):

$$f_U(\bar{U}) = \frac{k\bar{U}^{k-1}}{c^k}\exp\left[-\left(\frac{\bar{U}}{c}\right)^k\right] \tag{5.58}$$

The total damage from narrow-band vibration for all possible mean wind speeds is obtained from equations (5.49), (5.57) and (5.58) and integrating.

The fraction of the time *T* during which the mean wind speed falls between *U* and $U + \delta U$ is $f_U(U).\delta U$.

Hence the amount of damage generated while this range of wind speed occurs is from equations (5.49) and (5.57):

$$D_U = \frac{\nu_o^+ T f_U(U)\delta U}{K}(\sqrt{2}AU^n)^m\Gamma\left(\frac{m}{2}+1\right)$$

The total damage in time *T* during all mean wind speeds between 0 and ∞,

$$D = \frac{\nu_o^+ T(\sqrt{2}A)^m}{K}\Gamma\left(\frac{m}{2}+1\right)\int_0^\infty U^{mn} f_U(U)dU$$

$$= \frac{\nu_o^+ T(\sqrt{2}A)^m}{K}\Gamma\left(\frac{m}{2}+1\right)\int_0^\infty U^{mn+k-1}\frac{k}{c^k}\exp\left[-\left(\frac{U}{c}\right)^k\right]dU \tag{5.59}$$

This can be integrated numerically for general values of *k*. Usually *k* is around 2, in which case,

$$D = \frac{2\nu_o^+ T(\sqrt{2}A)^m}{Kc^2}\Gamma\left(\frac{m}{2}+1\right)\int_0^\infty U^{mn+1}\exp\left[-\left(\frac{U}{c}\right)^2\right]dU$$

This is now of the form of equation (5.50), so that:

$$D = \frac{2\nu_o^+ T(\sqrt{2}A)^m}{Kc^2}\Gamma\left(\frac{m}{2}+1\right)\frac{c^{mn+2}}{2}\Gamma\left(\frac{mn+2}{2}\right)$$

$$= \frac{\nu_o^+ T(\sqrt{2}A)^m c^{mn}}{K} \Gamma\left(\frac{m}{2}+1\right)\Gamma\left(\frac{mn+2}{2}\right) \tag{5.60}$$

This is a useful closed form expression for the fatigue damage over a lifetime of wind speeds, assuming narrow band vibration.

For wide band vibration, equation (5.60) can be modified, following equation (5.51), to:

$$D = \frac{\lambda \nu_o^+ T(\sqrt{2}A)^m c^{mn}}{K} \Gamma\left(\frac{m}{2}+1\right)\Gamma\left(\frac{mn+2}{2}\right) \tag{5.61}$$

By setting D equal to 1 in equations (5.60) and (5.61), we can obtain lower and upper limits to the fatigue life as follows:

$$T_{lower} = \frac{K}{\nu_o^+ (\sqrt{2}A)^m c^{mn} \Gamma\left(\frac{m}{2}+1\right)\Gamma\left(\frac{mn+2}{2}\right)} \tag{5.62}$$

$$T_{upper} = \frac{K}{\lambda \nu_o^+ (\sqrt{2}A)^m c^{mn} \Gamma\left(\frac{m}{2}+1\right)\Gamma\left(\frac{mn+2}{2}\right)} \tag{5.63}$$

Example

To enable the calculation of fatigue life of a welded connection at the base of a steel pole, using equations (5.62) and (5.63), the following values are assumed:

$m = 5$; $n = 2$; $\nu_0^+ = 1.0$ Hertz (the natural frequency of the pole) for the lower limit; 0.5 Hertz (one half the natural frequency) for the upper limit of fatigue life

$K = 2 \times 10^{15}$ [MPa]$^{1/5}$; $c = 8$ m/s; $A = 0.1 \dfrac{\text{MPa}}{(\text{m/s})^2}$

$$\Gamma\left(\frac{m}{2}+1\right) = \Gamma(3.5) = e^{1.201} = 3.323$$

$$\Gamma\left(\frac{mn+2}{2}\right) = \Gamma(6) = 5! = 120$$

Then from equation (5.62),

$$T_{lower} = \frac{2 \times 10^{15}}{1.0 \times (\sqrt{2} \times 0.1)^5 \times 8^{10} \times 3.323 \times 120.0}$$

$$= 0.826 \times 10^8 \text{ secs} = \frac{0.826 \times 10^8}{365 \times 24 \times 3600} \text{ years} = 2.62 \text{ years}$$

From equation (5.53), $a = 0.926 - 0.033\text{m} = 0.761$.

From equation (5.52), this is a lower limit for λ

$$T_{upper} = \frac{2T_{lower}}{\lambda} = \frac{5.24}{0.761} \text{ years} = 6.88 \text{ years}$$

This example illustrates the sensitivity of the estimates of fatigue life to the values of both A and c. For example, increasing A to $0.15\frac{\text{MPa}}{(\text{m/s})^2}$ would decrease the fatigue life by 7.6 times (1.5^5). Decreasing c from 8 to 7 m/s will increase the fatigue life by 3.8 times $(8/7)^{10}$.

5.7 Summary

This chapter has covered a wide range of topics relating to the dynamic response of structures to wind forces. For wind loading, the subresonant or background response should be distinguished from the contributions at the resonant frequencies and calculated separately.

The along-wind response of structures that can be represented as single- and multi-degree-of-freedom systems has been considered. The effective static load approach in which the distributions of the mean, background and resonant contributions to the loading are considered separately, and assembled as a combined effective static wind load, has been presented.

Aeroelastic effects such as aerodynamic damping, and the instabilities of galloping and flutter have been introduced. Finally wind-induced fatigue has been treated resulting in usable formulae for the calculation of fatigue life of a structure under along-wind loading.

Cross-wind dynamic response from vortex shedding has not been treated in this chapter, but is discussed in Chapters 9 and 11.

References

Ashraf Ali, M. and Gould, P. L. (1985) 'On the resonant component of the response of single degree-of-freedom systems under wind loading', *Engineering Structures* 7: 280–2.

Bendat, J. S. and Piersol, A. G. (1999) *Random Data: Analysis and Measurement Procedures*. 3rd edn. New York: J. Wiley.

Clough, R. W. and Penzien, J. (1975) *Dynamics of Structures*. New York: McGraw-Hill.

Crandall S. H. and Mark W. D. (1963) *Random Vibration in Mechanical Systems*. New York: Academic Press.

Davenport, A.G. (1961) 'The application of statistical concepts to the wind loading of structures', *Proceedings, Institution of Civil Engineers* 19: 449–71.

—— (1963) 'The buffetting of structures by gusts', *Proceedings, International Conference on Wind Effects on Buildings and Structures*, Teddington U.K., 26–8 June, 358–91.

—— (1964) 'Note on the distribution of the largest value of a random function with application to gust loading', *Proceedings, Institution of Civil Engineers* 28: 187–96.

—— (1967) 'Gust loading factors', *ASCE Journal of the Structural Division* 93: 11–34.

Dowling, N. E. (1972) 'Fatigue failure predictions for complicated stress-strain histories', *Journal of Materials* 7: 71–87.

Harris R. I. (1963) 'The response of structures to gusts', *Proceedings, International Conference on Wind Effects on Buildings and Structures*, Teddington U.K., 26–8 June, 394–421.

Holmes, J. D. (1994) 'Along-wind response of lattice towers. Part I: derivation of expressions for gust response factors', *Engineering Structures* 16: 287–92.

—— (1996a) 'Along-wind response of lattice towers. Part II: aerodynamic damping and deflections', *Engineering Structures* 18: 483–8.
—— (1996b) 'Along-wind response of lattice towers. Part III: effective load distributions', *Engineering Structures* 18: 489–94.
Holmes, J. D. and Best, R. J. (1981) 'An approach to the determination of wind load effects for low-rise buildings', *Journal of Wind Engineering and Industrial Aerodynamics* 7: 273–87.
Holmes, J. D. and Kasperski, M. (1996) 'Effective distributions of fluctuating and dynamic wind loads', *Civil Engineering Transactions, Institution of Engineers, Australia* CE38: 83–8.
Kasperski, M. and Niemann, H.-J. (1992) 'The L.R.C. (Load-Response-Correlation) method: a general method of estimating unfavourable wind load distributions for linear and non-linear structural behaviour', *Journal of Wind Engineering Industrial Aerodynamics* 43: 1753–63.
Matsuishi, M. and Endo, T. (1968) 'Fatigue of metals subjected to varying stress', *Japan Society of Mechanical Engineers Meeting*, Fukuoka, March.
Matsumoto, M. (1996) 'Aerodynamic damping of prisms', *Journal of Wind Engineering and Industrial Aerodynamics* 59: 159–75.
Rice, S. O. (1944–5) 'Mathematical analysis of random noise', *Bell System Technical Journal* 23: 282–332 and 24: 46–156. Reprinted in N. Wax, *Selected Papers on Noise and Stochastic Processes*, New York: Dover, 1954.
Scanlan, R. H. (1982) 'Developments in low-speed aeroelasticity in the civil engineering field', *A.I.A.A. Journal* 20: 839–44.
Scanlan, R. H. and Gade, R. H. (1977) 'Motion of suspended bridge spans under gusty winds', *ASCE. Journal of the Structural Division* 103: 1867–83.
Scanlan, R. H. and Tomko, J. J. (1971) 'Airfoil and bridge deck flutter derivatives', *ASCE Journal of the Engineering Mechanics Division* 97: 1717–37.
Vickery, B. J. (1965) 'On the flow behind a coarse grid and its use as a model of atmospheric turbulence in studies related to wind loads on buildings', National Physical Laboratory (U.K.) Aero Report 1143.
—— (1966) 'On the assessment of wind effects on elastic structures', *Australian Civil Engineering Transactions* CE8: 183–92.
—— (1995) 'The response of chimneys and tower-like structures to wind loading', in P. Krishna (ed.) *A State of the Art in Wind Engineering*, Wiley Eastern Limited.
Warburton, G. B. (1976) *The Dynamical Behaviour of Structures,* 2nd edn. Oxford: Pergamon Press Ltd.
Wirsching, P. H. and Light, M. C. (1980) 'Fatigue under wide band random stresses', *Journal of the Structural Division, A.S.C.E.* 106: 1593–607.